Fundamental behavior of electric field enhancements in the gaps between closely spaced nanostructures

Jeffrey M. McMahon, Stephen K. Gray, and George C. Schatz

Fundamental Behavior of Electric Field Enhancements in the Gaps Between Closely Spaced Nanostructures

Jeffrey M. McMahon,[1, 2] Stephen K. Gray,[2] and George C. Schatz[1]

[1]*Department of Chemistry, Northwestern University, Evanston, IL 60208*
[2]*Center for Nanoscale Materials, Argonne National Laboratory, Argonne, IL 60439*
(Dated: January 26, 2011)

We demonstrate that the electric field enhancement that occurs in a gap between two closely spaced nanostructures, such as metallic nanoparticles, is the result of a transverse electromagnetic waveguide mode. We derive an explicit semianalytic equation for the enhancement as a function of gap size, which we show has a universal qualitative behavior in that it applies irrespective of the material or geometry of the nanostructures and even in the presence of surface plasmons. Examples of perfect electrically conducting and Ag thin-wire antennas and a dimer of Ag spheres are presented and discussed.

PACS numbers: 78.67.-n, 62.23.Hj, 42.25.Fx, 42.25.Gy

I. INTRODUCTION

Structures that generate large electric field enhancements relative to the incident field, hereon referred to as $|\mathbf{E}|^2$ enhancements, have recently received a great deal of attention[1–10]. This is because such enhancements are central to a number of physical processes, including such surface-enhanced spectroscopy techniques as surface-enhanced Raman scattering (SERS), second harmonic generation, and enhanced absorption and fluorescence[1]. Often the enhanced field is generated in the small crevices of a roughened metal surface[2] or at the junctions of closely spaced nanoparticles[3–10]. Herein we focus on the latter structures, and while much is known about the $|\mathbf{E}|^2$ enhancements in them, there is still confusion over fundamental principles. In particular, the functional dependence on gap size[3,5,8,9], arguably the most basic and important aspect, has not been quantitatively determined and the underlying physical principles which determine it are not entirely known. It is the purpose of this paper to resolve this issue through finite element method (FEM) calculations[11] and an analytical theory developed for the transmission of light through an isolated slit in a metal film[12].

For two closely spaced nanostructures, the $|\mathbf{E}|^2$ enhancements in the resulting gap can in principle be explained using antenna theory[13,14], where the open-circuit voltage across the gap is responsible, and thus the systems are often classified as such[3,4]. We therefore begin by considering a two-dimensional (2D) antenna as shown schematically in Fig. 1. [The extension to three dimensions (3D) will be discussed below.] Two metal wires M with widths w are separated by a distance a and the entire structure spans a length of h. The structure is illuminated from below at normal incidence by a plane wave with wavelength λ, and we wish to determine how the $|\mathbf{E}|^2$ enhancement at the center of the gap depends on a. It is important to realize that for a real metal and distances less than approximately 1 nm, nonlocal dielectric effects will become important[15]. Our quantitative analysis herein will therefore be for $a \geq 1$ nm, but in most cases we will include smaller distances to highlight qualitative features. Antenna theory for a perfect electrically conducting (PEC) thin-wire antenna ($w \ll h$) assumes that the incident electric field $\mathbf{E}_0$ generates an alternating current along x, which results in an induced voltage V across h. If $h \approx n\lambda/2$, where n is an integer, the antenna resonates and $V \approx -E_0 h$, where E_0 is the amplitude of the incident field[13]. As a result, the open-circuit voltage in the gap should produce a uniform $|\mathbf{E}|^2$ enhancement of $|\mathbf{E}|^2/|\mathbf{E}_0|^2 = |V/a|^2/|E_0|^2 \approx h^2/a^2$. (Note that this estimate ignores coupling between the gap and antenna ends that when rigorously included leads to a slightly weaker a-dependence than $1/a^2$.)
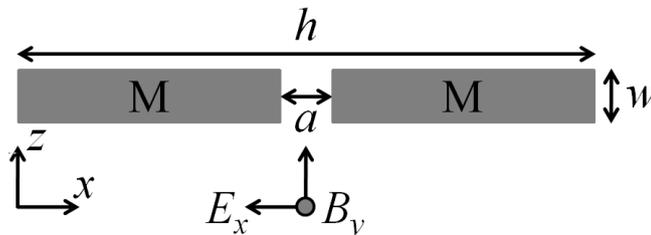

FIG. 1: Schematic diagram of a thin-wire antenna. The parameters shown are discussed in the text.
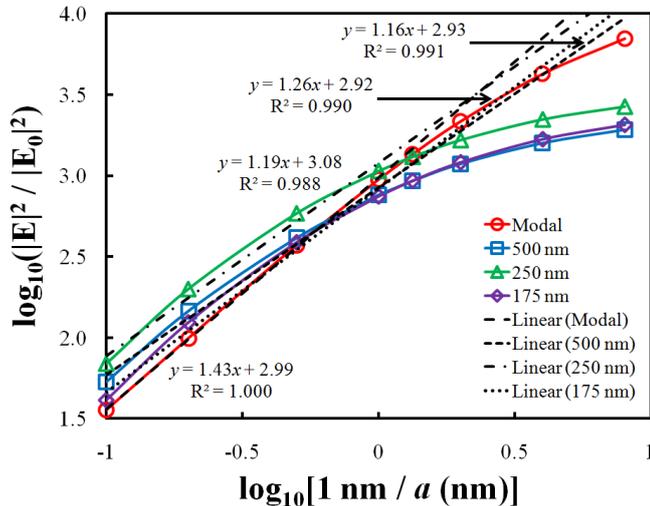
FIG. 2: $|\mathbf{E}|^2$ enhancements as a function of gap size for PEC thin-wire antennas with parameters given in the text. Solid lines are used to connect the actual data points (symbols).

In order to test the above analysis, we rigorously determined the $|\mathbf{E}|^2$ enhancements via FEM calculations[11] for $h = 250$ and 500 nm thin-wire antennas ($n = 1$ and 2, respectively) with $w = 5$ nm at $\lambda = 500$ nm for gap sizes of $a = 0.125$ to 10 nm. To characterize the a dependence, we can assume that $|\mathbf{E}|^2/|\mathbf{E}_0|^2$ is proportional $1/a^p$ and plot the results on a $\log_{10}$-$\log_{10}$ scale to determine p; Fig. 2. For both antennas it is found that $p \approx 1.2$ for $a \geq 1$ nm, and it is even less for smaller a, which is much lower than the above antenna theory prediction of $p = 2$. An alternative way to describe these systems and the $|\mathbf{E}|^2$ enhancements that they exhibit is therefore needed.

II.   THEORETICAL FRAMEWORK

The system in Fig. 1 can be greatly simplified by taking $h \to \infty$, which below we will show does not significantly affect the behavior of the electric field $\mathbf{E}$ in the gap. Maxwell's equations can be solved analytically for such a system (if the metal is a PEC), which is an isolated slit in a metal film, by appropriately expanding the transverse component of the field (the y component of the magnetic field, in this case) above and below the film and inside of the gap in terms of known functions and applying boundary conditions at the interfaces. While the full solution for this problem has been implicitly worked out in terms of a system of linear equations[12], we demonstrate that under a few reasonable approximations it is possible to obtain a tractable semianalytical form for $|\mathbf{E}|^2/|\mathbf{E}_0|^2$.

Inside the gap $\mathbf{E}$ can be defined entirely in terms of its x component E_x (below we will show that the z component E_z is zero), which can be expanded as a superposition of forward and backwards propagating (and evanescent) waveguide modes m,

$$E_x(x,z) = \sum_{m=0}^{\infty} \frac{\beta_m}{k_0} \left(A_m e^{i\beta_m z} - B_m e^{-i\beta_m z} \right) \phi_m(x) \ , \tag{1}$$

where A_m and B_m are the respective modal amplitudes, $k_0 = 2\pi/\lambda$, $\beta_m = \left[k_0^2 - (m\pi/a)^2 \right]^{1/2}$, and $\phi_m(x) = \left(2/a^{1/2}\right) \cos\left[m\pi\left(x + a/2\right)/a\right]$ is the solution to the Helmholtz equation subject to PEC boundary conditions on the gap sides at $x = \pm a/2$. A_m and B_m can be found by ensuring the continuity of Eq. (1) at the input (I) and output (O) surfaces of the gap,

$$A_m = \frac{1}{2} \frac{k_0}{\beta_m} E_m^I \left\{ 1 + i \left[\frac{1}{\tan(\beta_m w)} - \frac{E_m^O/E_m^I}{\sin(\beta_m w)} \right] \right\} \tag{2}$$

$$B_m = \frac{1}{2} \frac{k_0}{\beta_m} E_m^I \left\{ -1 + i \left[\frac{1}{\tan(\beta_m w)} - \frac{E_m^O/E_m^I}{\sin(\beta_m w)} \right] \right\} \tag{3}$$

where E_m^I and E_m^O are intensities of scattering events that take place at each of the surfaces, which can be determined by solving a set of linear equations (see below)[12].

Inside a gap that is small relative to the incident wavelength ($k_0 a \ll 1$), the only waveguide mode that can exist is the $m = 0$ transverse electromagnetic (TEM) one[16]. In this case, there is no x dependence in E_x, E_z is zero, $\beta_0 = k_0$, and the linear equations defining E_0^I and E_0^O simplify considerably,

$$E_0^I = I_0 \frac{f_0 + g_{00}}{(f_0 + g_{00})^2 - (g_0^v)^2} \tag{4}$$

$$E_0^O = -\frac{g_0^v}{f_0 + g_{00}} E_0^I \tag{5}$$

where $I_0 = 4E_0 a^{1/2}$ (for normal incident light) is the overlap amplitude of the incident field with the TEM mode, $f_0 = i \cot (k_0 w)$ is the admittance amplitude, $g_0^v = i \csc (k_0 w)$ is the coupling amplitude between I and O, and

$$g_{00} = \frac{4}{a} \int_{-a/2}^{a/2} \int_{-a/2}^{a/2} dx \ dx' \ G(x, x') \tag{6}$$

is the amplitude of the TEM mode's self-interaction, where $G(x, x') = (k_0/2) H_0^{(1)} (k_0 |x - x'|)$ is the 2D vacuum Green's function with $H_0^{(1)}$ being a Hankel function of the first kind. The maximum value that $k_0 |x - x'|$ can take is $k_0 a$. Since $k_0 a \ll 1$, we can make the small-argument approximation in $H_0^{(1)}$ and perform the integral in Eq. (6) analytically,

$$g_{00} = 2k_0 a (1 + il) \tag{7}$$

where $l = (2/\pi) [\ln (k_0 a/2) + \gamma - 3/2]$ with γ being Euler's constant.

For a gap with a small width relative to the incident wavelength ($k_0 w \ll 1$) we can use the small-angle approximation in Eqs. (2) and (3) to greatly simplify Eq. (1),

$$E_x(z) = 8E_0 \frac{f_0 + g_{00}}{(f_0 + g_{00})^2 - (g_0^v)^2} \left[1 - \frac{z}{w} \left(1 - \frac{f_0}{f_0 + g_{00}} \right) \right] \quad . \tag{8}$$

Note that the approximation $g_{00} \ll 2f_0$ was also used to get Eq. (8), which is valid considering that the leading terms are $k_0 a$ and $1/k_0 w$, respectively.

At the center of the gap ($z = w/2$) Eq. (8) simplifies even further,

$$E_x(w/2) = 8E_0 \frac{1}{2g_{00} + u} \tag{9}$$

where $u = f_0 - (g_0^v)^2 / f_0 = -i \tan (k_0 w) \approx -i k_0 w$. Equation (9) shows that at the center of the gap $\mathbf{E}$ is inversely proportional to the interference between two terms, the self-interaction term g_{00}, which depends only on $k_0 a$, and a term u representing the interference between surfaces I and O, which depends only on $k_0 w$.

Using the explicit expressions for g_{00} and u in Eq. (9) and calculating $|\mathbf{E}|^2/|\mathbf{E}_0|^2$ gives

$$|\mathbf{E}|^2/|\mathbf{E}_0|^2 = |E_x(w/2)|^2/|E_0|^2 = \frac{64}{16 (1 + l^2) (k_0 a)^2 + 8l (k_0 a) (k_0 w) + (k_0 w)^2} \quad . \tag{10}$$

Note that Eq. (10) is in terms of the dimensionless quantities $k_0 a$ and $k_0 w$. Since our focus is on the dependence of $|\mathbf{E}|^2$ with a, we will consider cases in which k_0 and w are kept fixed.

III. APPLICATIONS

For gaps with a not very small relative to w (greater than approximately 1 nm for the thin-wire antennas discussed above), $\mathbf{E}$ depends primarily on g_{00} and $|\mathbf{E}|^2/|\mathbf{E}_0|^2 \approx 64/\left[16 (1 + l^2) (k_0 a)^2 \right]$. Because the enhancement is of the form $1/l^2 a^2$, we would expect a $1/a^p$ fit to not work at all. However, over a couple order of magnitude range of a values $l \sim \ln (k_0 a/2)$ is well-approximated by $A (k_0 a/2)^b$, where A and b are constants that can be determined by demanding
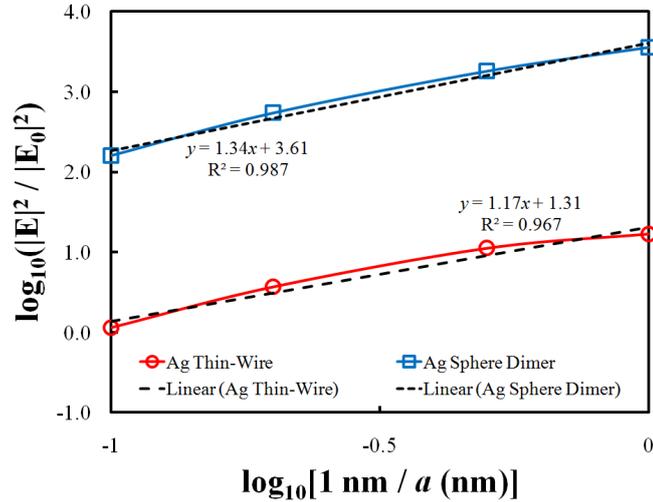
FIG. 3: $|\mathbf{E}|^2$ enhancements as a function of gap size for a 3D Ag thin-wire antenna and a dimer of Ag spheres with parameters given in the text. Solid lines are used to connect the actual data points (symbols).

that this equality and a corresponding one involving its derivative be satisfied at some value of $k_0 a/2$. With these constraints one finds that $b = 1/\ln(k_0 a/2)$, which varies slowly with $k_0 a/2$. For $\lambda = 500$ nm and $1 \leq a \leq 10$ nm, $b \approx -0.25$ and therefore $1/l^2 a^2 \sim 1/a^{1.5}$, which is consistent with $p \approx 1.2$ found for the thin-wire antennas in Fig. 2. For small gaps both a^2 and $l^2 a^2$ go to zero, which means that $\mathbf{E}$ depends primarily on u and $|\mathbf{E}|^2/|\mathbf{E}_0|^2 \approx 64/(k_0 w)^2$. Therefore, for $a \ll w$ we expect a turnover to a weaker $1/a^p$ dependence, which is also consistent with the results in Fig. 2. Actual $|\mathbf{E}|^2$ enhancements calculated using Eq. (10) for $a = 0.125$ to 10 nm, $w = 5$ nm, and $\lambda = 500$ nm are shown in Fig. 2 as well, and are in agreement with these remarks.

The strong agreement between the modal and thin-wire antenna results in Fig. 2 suggests that the $|\mathbf{E}|^2$ enhancements in both cases arise from the same effect, a TEM waveguide mode. The former does show a slightly stronger $1/a^p$ dependence, but this can be understood as follows. Recall that the amplitude for coupling incident light into this mode is proportional to their overlap; see Eq. (4). In a finite structure, such as a thin-wire antenna, some of the impinging incident light can be effectively lost via scattering, leading to a less efficient coupling into the TEM mode and a weaker $1/a^p$ dependence. Quantitatively, the amount of scattering is given by the scattering efficiency Q_{sc} (the ratio of the scattering cross section to the geometric one). In the modal results Q_{sc} is naturally 0, since the geometric cross section is infinite. For a finite structure, however, $Q_{sc} \geq 0$. For example, the resonant antennas $h = 500$ and 250 nm have similar Q_{sc} values of 1.953 and 1.915, respectively, at $a = 2$ nm. For an off-resonance condition we expect less scattering, and in fact this is what is numerically found for $h = 175$ nm. In this case, $Q_{sc} = 0.931$ nm (at $a = 2$ nm) and the $1/a^p$ dependence is indeed stronger than for the two resonant antennas.

Thusfar we have considered 2D systems. While such structures are experimentally realizable, in most cases (e.g., typical SERS substrates) structures are 3D in character. Nonetheless, our analysis remains valid and Eq. (10) should still apply (qualitatively, at least). This is because the TEM waveguide mode suggested as responsible for the $|\mathbf{E}|^2$ enhancements also exists in 3D. The only requirement to support a propagating electromagnetic wave is that an oscillating potential difference be established between the walls supporting the wave (e.g., the sides of a gap)[17]. In addition to 3D, actual structures are comprised of a real metal, typically Ag or Au at optical frequencies due to possible increases in $|\mathbf{E}|^2$ enhancements via surface plasmon (SP) excitations[7,10]. Furthermore, such structures often have a more complex geometry than a pair of thin wires. Neither of these issues are addressed directly by Eq. (10). Although, based on the discussion above about Q_{sc}, it is reasonable to suspect that the dominant effect of both of these issues is that there may be wavelength dependent modulations to the $1/a^p$ dependence, due to corresponding dependencies in the absorption efficiency (Q_{abs}) and Q_{sc} on both the material and geometry of the structures[18]. However, the overall trends and underlying physical principles should remain the same, which we confirm below.

As a first example of the applicability of our analysis to real 3D structures, FEM was used to calculate the $1/a^p$ dependence at the center of a 3D Ag thin-wire antenna with $h = 250$ nm and $w = 5$ nm (both in and out of the plane of Fig. 1) at $\lambda = 500$ nm; Fig. 3. It is found that p is again approximately 1.2, which is nearly equal to the analogous 2D PEC thin-wire antenna results in Fig. 2 and is consistent with a recent experimental and numerical study of the a-dependence in Au bowtie structures[19]. Further similarity to the PEC results comes from the behavior as a decreases, where the $1/a^p$ dependence again becomes weaker, as can be inferred from the curvature of the actual data relative to the linear fit. Interestingly, Fig. 3 shows that the actual magnitude of $|\mathbf{E}|^2$ for the Ag thin-wire antenna
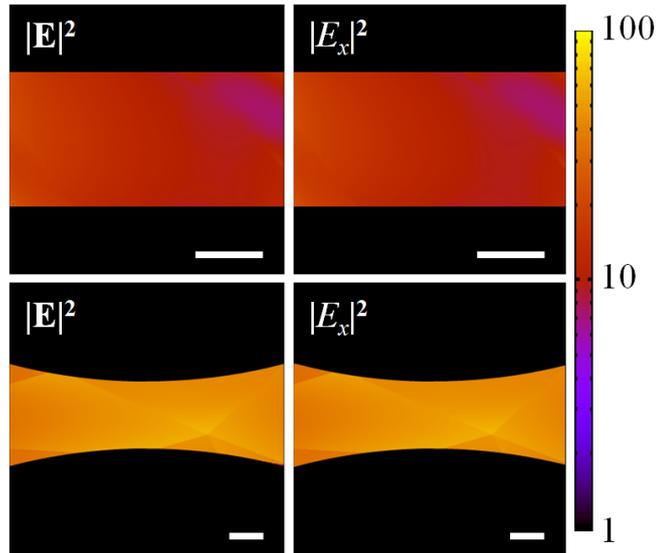
FIG. 4: Intensities of $|\mathbf{E}|^2$ and the incident component of $\mathbf{E}$, $|E_x|^2$, in the gaps of a 3D Ag thin-wire antenna (top) and Ag sphere dimer (bottom) with parameters discussed in the text. The inset white scale bars correspond to 1 nm. Note that the intensity values have been rescaled relative to Fig. 3 to fit clearly on the same scale, and the fields inside of the structures have been set to 0.

is lower than the analogous PEC one (Fig. 2). Nonetheless, in both cases once the magnitude of $|\mathbf{E}|^2$ is known for a particular value of a Eq. (10) can be used to accurately calculate the magnitude at any other value.

It is possible to verify the existence of a TEM waveguide mode by looking at profiles of $\mathbf{E}$ inside the gap, as for normal incident linearly-polarized light this mode has the same polarization. Figure 4 shows the fields inside the gap of the antenna discussed above for $a = 2$ nm, and it can be seen that this is indeed the case, as $|\mathbf{E}|^2 \approx |E_x|^2$. (Note that $|E_y|^2$ and $|E_z|^2$ are both less than 1 on the scale in Fig. 4.) In fact, it has recently been demonstrated experimentally that electromagnetic fields inside the gaps of nanostructures are linearly polarized, even in more complex ones than discussed here[20]. In the context of plasmonics, the fundamental waveguide mode is often referred to as a gap-plasmon[21–23]. However, it is important to note that Figs. 2 – 4 demonstrate that the mode under discussion does not depend on the existence of surface plasmons.

As a further and final example of the applicability of our analysis to real 3D structures, $|\mathbf{E}|^2$ enhancements as a function of gap size were calculated for a dimer of 250 nm diameter Ag spheres at $\lambda = 633$ nm (a popular type of experimental system and common laser wavelength[6]); Fig. 3. The $1/a^p$ dependence in this case is found to be characterized by $p \approx 1.3$, which is nearly equal to the modal result of $p \approx 1.4$, and slightly greater than the somewhat analogous thin-wire antenna result in Fig. 3. The stronger $1/a^p$ dependence is related to the fact that this structure is more efficient for capturing light[18], as indicated by $Q_{\mathrm{abs}} = 0.200$ as opposed to 0.087 for the thin-wire antenna, for example. Field profiles inside the gap again indicate the presence of a TEM waveguide mode; Fig. 4. Looking closely at Fig. 3 reveals that there is a much less strong turnover to a weaker $1/a^p$ dependence for smaller a than was seen for any of the other structures. Such behavior is understandable considering that w is effectively zero in this case (there is only a single point of minimum approach), which can lead to $|\mathbf{E}|^2$ being unbounded as $a \to 0$ $[\lim_{a\to 0} \left(1 + l^2\right) \left(k_0 a\right)^2 = 0$; see Eq. (10)]. It is quite remarkable that the simple analysis derived for a 2D PEC film with an isolated slit is so accurate when applied to full 3D structures of other geometries, and even in the presence of SPs.

IV. SUMMARY

In summary, through a combination of semianalytical analysis and numerical calculations we explored the fundamental behavior of $|\mathbf{E}|^2$ enhancements that occurs in the gaps between closely spaced nanostructures. We demonstrated a universal behavior in the variation with gap size a of the form $1/a^p$ with $p \approx 1.2 - 1.5$, which is weaker than the result expected based on simple antenna theory arguments of $1/a^2$. Furthermore, we demonstrated that the confined fields always display characteristics of a TEM waveguide mode. These general features were shown to occur irrespective of the geometry of the nanostructures, and are applicable to both perfect conductors as well as metals that

support surface plasmons. These results should prove useful for a fundamental undertanding of $|\mathbf{E}|^2$ enhancements and applications that depend critically on them, such as SERS.

Acknowledgments

1 M. Moskovits, Rev. Mod. Phys. **57**, 783 (1985).
2 F. J. García-Vidal and J. B. Pendry, Phys. Rev. Lett. **77**, 1163 (1996).
3 P. J. Schuck, D. P. Fromm, A. Sundaramurthy, G. S. Kino, and W. E. Moerner, Phys. Rev. Lett. **94**, 017402 (2005).
4 P. Mühlschlegel, H.-J. Eisler, O. J. F. Martin, B. Hecht, and D. W. Pohl, Science **308**, 1607 (2005).
5 J. H. Kang, D. S. Kim, and Q.-H. Park, Phys. Rev. Lett. **102**, 093906 (2009).
6 K. L. Wustholz, A.-I. Henry, J. M. McMahon, R. G. Freeman, N. Valley, M. E. Piotti, M. J. Natan, G. C. Schatz, and R. P. Van Duyne, J. Am. Chem. Soc. **132**, 10903 (2010).
7 E. Hao and G. C. Schatz, J. Chem. Phys. **120**, 357 (2004).
8 J. Aizpurua, G. W. Bryant, L. J. Richter, F. J. García de Abajo, B. K. Kelley, and T. Mallouk, Phys. Rev. B **71**, 235420 (2005).
9 I. Romero, J. Aizpurua, G. W. Bryant, and F. J. García de Abajo, Opt. Express **14**, 9988 (2006).
10 J. P. Kottmann and O. J. F. Martin, Opt. Express **8**, 655 (2001).
11 J. Jin, *The Finite Element Method in Electromagnetics* (John Wiley & Sons, Inc.: New York, 2002), 2nd ed.
12 J. Bravo-Abad, L. Martín-Moreno, and F. J. García-Vidal, Phys. Rev. E **69**, 026601 (2004).
13 J. D. Kraus and R. J. Marhefka, *Antennas* (McGraw-Hill Education: Singapore, 2001), 3rd ed.
14 D. W. Pohl, in *Near-Field Optics: Principles and Applications*, edited by M. Ohtsu and X. Zhu (World Scientific: Singapore, 2000).
15 J. M. McMahon, S. K. Gray, and G. C. Schatz, Phys. Rev. Lett. **103**, 097403 (2009).
16 J. D. Jackson, *Classical Electrodynamics* (John Wiley & Sons, Inc.: New York, 1998), 3rd ed.
17 J. C. Slater and N. H. Frank, *Electromagnetism* (Dover Publications, Inc.: New York, 1969).
18 C. F. Bohren and D. R. Huffman, *Absorption and Scattering of Light by Small Particles* (John Wiley & Sons, Inc.: New York, 1983).
19 N. A. Hatab, C.-H. Hsueh, A. L. Gaddis, S. T. Retterer, J.-H. Li, G. Eres, Z. Zhang, and B. Gu, Nano Lett. **10**, 4952-4955 (2010).
20 M. Schnell, A. Garcia-Etxarri, J. Alkorta, J. Aizpurua, and R. Hillenbrand, Nano Lett. **10**, 3524-3528 (2010).
21 S. A. Maier, *Plasmonics: Fundamentals and Applications* (Springer: New York, 2007).
22 B. Prade, J. Y. Vinet, and A. Mysyrowicz, Phys. Rev. B **44**, 13556-13572 (1991).
23 H. T. Miyazaki and Y. Kurokawa, Phys. Rev. Lett. **96**, 097401 (2006).